Journal of Solid State Chemistry 184 (2011) 387–390

Contents lists available at ScienceDirect

Journal of Solid State Chemistry

journal homepage: www.elsevier.com/locate/jssc

Improve the catalytic activity of α-Fe_2O_3 particles in decomposition of ammonium perchlorate by coating amorphous carbon on their surface

Yifu Zhang [a], Xinghai Liu [b,*], Jiaorong Nie [c], Lei Yu [a], Yalan Zhong [a], Chi Huang [a,*]

[a] Engineering Research Center of Organosilicon Compound and Material, Ministry of Education of China, College of Chemistry and Molecular Sciences, Wuhan University, Wuhan 430072, PR China
[b] School of Printing and Packaging, Wuhan University, Wuhan 430079, PR China
[c] Jianghe Chemical Factory of CSSG, Yuan'an 444200, PR China

ARTICLE INFO

Article history:
Received 25 July 2010
Received in revised form
24 November 2010
Accepted 1 December 2010
Available online 7 December 2010

Keywords:
Nanocomposites
Nanomaterials
Core–shell
α-Fe_2O_3@C
α-Fe_2O_3
Ammonium perchlorate

ABSTRACT

Sphere- and pod-like α-Fe_2O_3 particles have been selectively synthesized using $NH_3 \cdot H_2O$ and NaOH solution to adjust the pH value of the designed synthetic system, respectively. The sphere-like α-Fe_2O_3 particles with diameter about 25 nm on average were encapsulated into carbon shells to fabricate a novel core–shell composite (α-Fe_2O_3@C) through the coating experiments. The catalytic performance of the products on the thermal decomposition of ammonium perchlorate (AP) was investigated by thermal gravimetric analyzer (TG) and differential thermal analysis (DTA). The thermal decomposition temperatures of AP in the presence of pod-like α-Fe_2O_3, sphere-like α-Fe_2O_3 and α-Fe_2O_3@C are reduced by 72, 81 and 109 °C, respectively, which show that α-Fe_2O_3@C core–shell composites have higher catalytic activity than that of α-Fe_2O_3.

1. Introduction

In past decades, core–shell nanostructures have been paid more and more attentions owing to their tunable surface properties, which can enhance their magnetic, electronic, optical and catalytic properties [1]. The core–shell materials may retain the properties of both cores and shells, which could afford composite properties in one system. Consequently, these novel materials have potential applications in diverse technological fields such as semiconductor electronics and biomedical industries [1–4]. Recently, core–shell structured nanoparticles with a carbon shell have stimulated great interest. A series of work has been focused on the synthesis of metal@C and metal oxides@C core–shell composites (e.g. Ag@C, Fe_3O_4@C, V_2O_3@C, etc.), and most of these new unique materials with amorphous carbon show some novel properties, which have been widely applied to lithium ion battery and catalyst [5–9]. However, to our best knowledge, the introduction of this amorphous carbon containing aromatic structures into the catalytic decomposition of ammonium perchlorate (AP) has not been reported. As is well known, AP is one of the most common oxidizing agents that have been used in various propellants and its thermal decomposition characteristics influence the combustion behavior of the solid propellant directly. The catalytic activities of some catalysts in the thermal decomposition of an AP have been reported and it was found that catalytic performance can be improved by the nanometer-scale catalysts [10–13]. Recent researches indicate that ferric oxides are proved to be quite effective on the thermal decomposition of AP [14–16]. In this paper, we will introduce the novel amorphous carbon containing aromatic structures as shells to enhance the catalytic activities of ferric oxides in the decomposition of AP.

Herein, we reported that the sphere- and pod-like α-Fe_2O_3 particles were selectively synthesized by a facile hydrothermal approach. Then, α-Fe_2O_3@C core–shell nanocomposites were prepared using the as-obtained sphere-like α-Fe_2O_3 as the cores and glucose as the resources of carbon by an environmental hydrothermal method. At last, all of the above products were mixed with AP and their catalytic performances on the thermal decomposition of AP were investigated by DTA. The results revealed that the α-Fe_2O_3@C core–shell composites have much higher catalytic activity on the thermal decomposition of AP than that of only α-Fe_2O_3.

2. Experimental section

2.1. Synthesis of sphere- and pod-like α-Fe_2O_3 nanoparticles

All the reagents purchased from Sinopharm Chemical Reagent Co., Ltd. were of analytic grade and used without any further purification. In a typical procedure, 3.00 g of $FeCl_3$, 4.67 g of $H_2C_2O_4 \cdot 2H_2O$, 20 mL of distilled water (H_2O) and 1.68 g of cetyltriethylammnonium bromide (CTAB: $C_{19}H_{42}BrN$) were orderly added into

* Corresponding authors. Fax: +86 27 68754067.
E-mail addresses: liuxh@whu.edu.cn (X. Liu), chihuang@whu.edu.cn (C. Huang).

0022-4596/$ - see front matter © 2010 Elsevier Inc. All rights reserved.
doi:10.1016/j.jssc.2010.12.004

a 50 mL of beaker and mixed with vigorously magnetic stirring for 30 min. Then, $NH_3 \cdot H_2O$ (10 wt%) or NaOH (10 wt%) was added dropwise to adjust the pH value under continuous stirring. After the pH value was adjusted to about 4, all the suspension were transferred into a 40 mL teflon lined stainless steel autoclave, which was sealed and maintained at 100 °C for 24 h. After cooling to room temperature naturally, the samples were filtered off, washed with distilled water and absolute ethanol several times and dried in vacuum at 75 °C for 12 h. Finally, α-Fe_2O_3 nanoparticles were obtained by calcining the above samples at 300 °C for 6 h in air atmosphere.

2.2. Synthesis of α-Fe_2O_3@C core–shell nanocomposites

To synthesize α-Fe_2O_3@C core–shell structure, the sphere-like α-Fe_2O_3 nanoparticles with small diameter were selected due to their large specific surface. In the experiment, 0.32 g of the as-obtained α-Fe_2O_3 nanoparticles were dispersed into 20 mL of distilled water by ultrasonic wave for 10 min. In order to modify the surface of α-Fe_2O_3 nanoparticles and improve the coated process, the diluted HNO_3 was dropped slowly to adjust the pH value to about 3 [3]. After the mixture was filtered off, the substrate solid was dispersed into the glucose solution (4.00 g of glucose and 30 mL of distilled water) under ultrasonic wave for 30 min. The suspension was transferred into a 40 mL teflon lined stainless steel autoclave, which was sealed and maintained at 180 °C for 4 h. After cooling to room temperature naturally, the samples were filtered off, washed with distilled water and absolute ethanol several times, and dried in vacuum at 75 °C for 12 h. Finally, α-Fe_2O_3@C core–shell nanoparticles were obtained by calcining the above samples at 500 °C for 2 h in N_2 atmosphere.

2.3. Characterization

The purity and crystalline structure of the resulting products were investigated by the X-ray powder diffraction (XRD, D8 X-ray diffractometer equipment with Cu $K\alpha$ radiation, $\lambda = 1.54060$ Å). The Raman spectrum was collected on a RM-1000 spectrometer with an argon-ion laser at an excitation wavelength of 514.5 nm. The chemical composition of the as-obtained samples was revealed by use of an energy-dispersive X-ray spectrometer (EDX) attached to a scanning electron microscope (SEM; Quanta 200). The morphologies of the products were observed by the transmission electron microscopy (TEM, JEM-100CXII). The elemental analysis (EA) of the samples was carried out using Vario EL III equipment (Germany) with TCD detector to analyze the element of C, H, N and S. Fourier transform infrared spectroscopy (FT-IR) pattern was recorded on Nicolet 60-SXB spectrometer from 4000 to 400 cm^{-1} with a resolution of 4 cm^{-1}. Thermo-gravimetric analysis and differential thermal analysis (TG/DTA) measurements were performed on Diamond TG-DTA 6300 at a heating rate of 10 °C min^{-1} in N_2 atmosphere in the range of 25–500 °C with Al_2O_3 as reference. The homogeneous mixture of product and AP was used for the DTA experiment, and the mass ratios of products to AP were 3:97.

3. Results and discussion

Fig. 1 shows the typical XRD patterns of the resulting products. All the diffraction peaks in Fig. 1a and b can be readily indexed as the rhombohedral crystalline phase (space group $R\text{-}3c$) of α-Fe_2O_3 with calculated lattice parameters $a = 5.026$, $c = 13.752$, which corresponds to (JCPDS, no. 89-596) already described in the literature [17]. No peaks of any other phases are detected from the XRD pattern, indicating the as-prepared α-Fe_2O_3 particles are of high purity. All the diffraction peaks in Fig. 1c could be readily indexed as rhombohedral α-Fe_2O_3, revealing that the crystalline phase is pure α-Fe_2O_3. However, the broadened peak ranging 15–30° can also be observed, which is attributed to amorphous

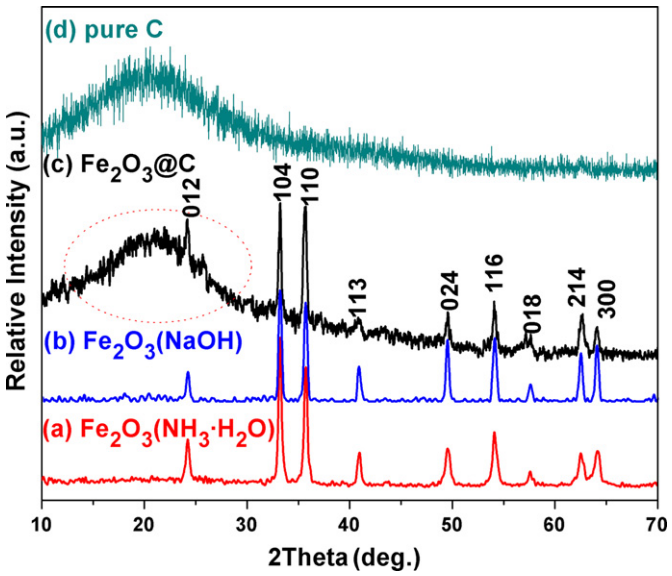

Fig. 1. XRD patterns of the products: (a) sphere-like α-Fe_2O_3 nanoparticles with $NH_3 \cdot H_2O$ adjusting pH; (b) pod-like α-Fe_2O_3 nanoparticles with an NaOH adjusting pH; (c) α-Fe_2O_3@C core–shell composites; and (d) pure carbon.

carbon [3]. Furthermore, the disorganized background results from amorphous carbon coating on the surface of α-Fe_2O_3 compared Fig. 1c with Fig. 1d. These results reveal that the as-synthesized product might be α-Fe_2O_3@C core–shell composites. Further information about the structure of the carbon shell coating on the surface of α-Fe_2O_3 was investigated by Raman spectrum, which was represented in Fig. S1 (*Supplementary data*). A typical Raman spectrum of α-Fe_2O_3@C core–shell composites exhibits two main peaks. The peaks located at 1360 cm^{-1} (D-band) and 1599 cm^{-1} (G-band) are attributed to the in-plane vibration of the disordered amorphous carbon and the in-plane vibrations of the crystalline graphite, respectively, which are the same as those of amorphous carbon [6,18]. The D-band is relatively high, further proving that the coating comprises disordered carbon. Therefore, the Raman spectrum shows that the carbon in α-Fe_2O_3@C sample is disordered, in agreement with the XRD pattern observations.

Fig. 2 represents the typical TEM images of the as-synthesized α-Fe_2O_3 nanoparticles and α-Fe_2O_3@C core–shell composite. When the pH value is adjusted by $NH_3 \cdot H_2O$, the morphology of the α-Fe_2O_3 nanoparticles is a sphere with diameter about 25 nm on an average, as shown in Fig. 2a and b. However, the pod-like α-Fe_2O_3 particles with the major axis of about 314 nm and the minor axis about 138 nm on an average (Fig. 2c) are synthesized when the pH value is adjusted by an NaOH solution. Thus, α-Fe_2O_3 particles with different morphologies are obtained using $NH_3 \cdot H_2O$ and NaOH to adjust the pH value. As is well known, $NH_3 \cdot H_2O$ is a weak base, while NaOH is a strong base, which might be the reason that the sphere- and pod-like α-Fe_2O_3 particles have been selectively synthesized. The TEM images of α-Fe_2O_3@C core–shell composites are shown in Fig. 2d and e. We can observe that the samples consist of well-dispersed particles with an average size ranging 30–50 nm, and the contrast grade between core and shell could even be observed, implying that the core–shell structure (inset Fig. 2d and e) has been formed. The deep background is α-Fe_2O_3, while the shallow background is amorphous carbon with thickness of about 12 nm on average. It is worth noting that, after the coating process, the core–shell particles scatter relatively better than that of sphere-like α-Fe_2O_3 particles and the as-synthesized α-Fe_2O_3@C core–shell materials are slightly cross-linked. It is their surface coated the colloidal carbon that contain lots of active function groups, which is in accordance with the FT-IR result discussed in the following section. The possible formation mechanism of α-Fe_2O_3@C core–shell

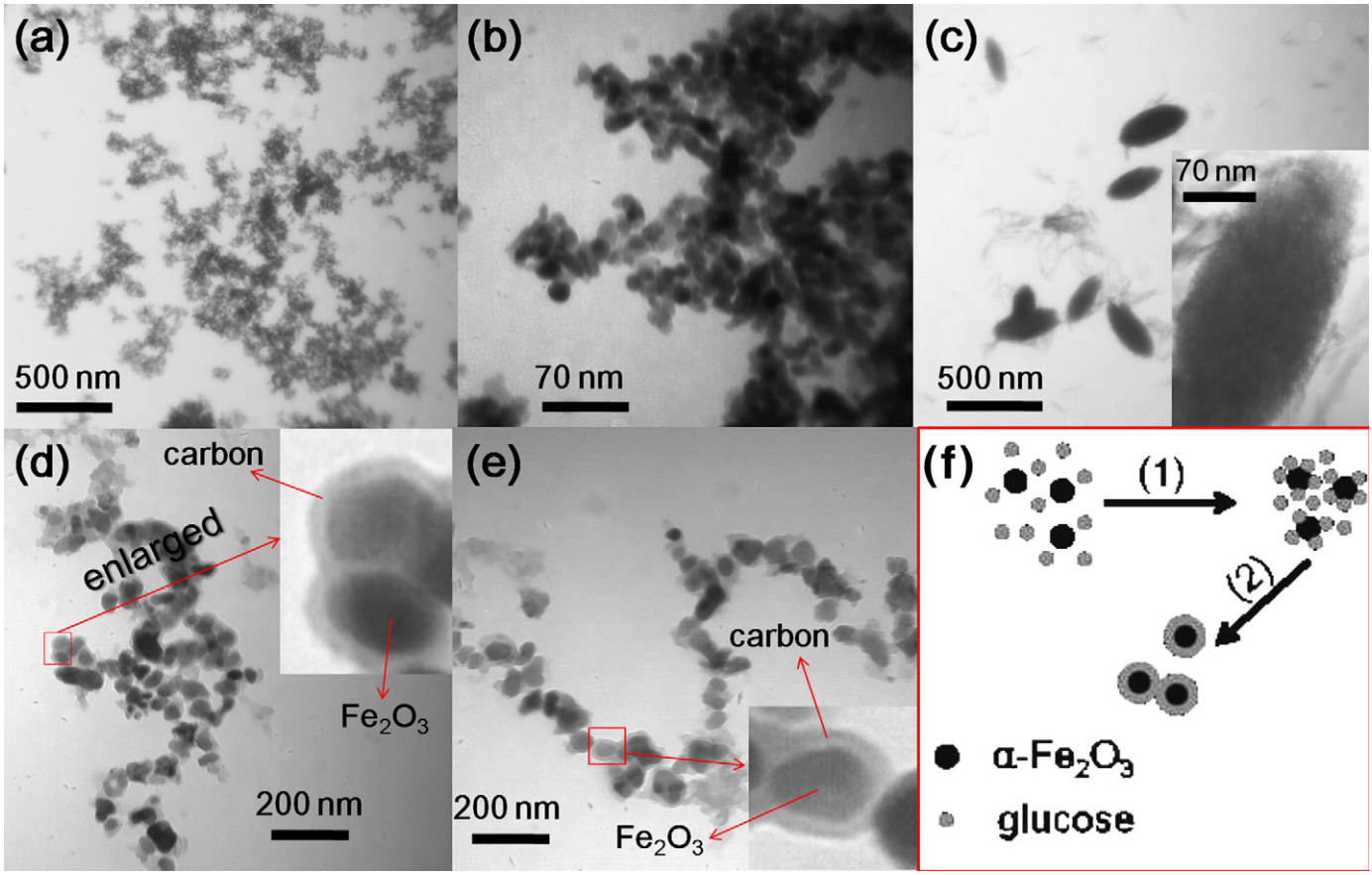

Fig. 2. (a) and (b) TEM images of α-Fe_2O_3 with $NH_3 \cdot H_2O$ adjusted the pH value; (c) TEM image of α-Fe_2O_3 with NaOH adjusted the pH value; (d) and (e) TEM images of α-Fe_2O_3@C core–shell composites, inset enlarged drawings; and (f) schematic illustration of the synthesis of α-Fe_2O_3@C core–shell structure.

composites is schematically illustrated in Fig. 2f. First, α-Fe_2O_3 particles are dispersed into the glucose solution. Then, the glucose molecules are absorbed on the surface of α-Fe_2O_3 particles. This process can be due to the surface of α-Fe_2O_3 particles containing some active function groups after diluted HNO_3 modifying, which is similar with the synthesis of Fe_3O_4@C [3]. Last, the glucose is undergoing dehydration, polymerization and carbonization, leading to the amorphous carbon with aromatic structure is finally formed on the surface of α-Fe_2O_3 particles, in agreement with the formation of colloidal carbon spheres [19].

More information about the composition of the core–shell structured materials was collected by the EDX, EA and FT-IR measurements. The typical EDX spectrum of α-Fe_2O_3@C core–shell composite was shown in Fig. S2 (*Supplementary data*), while it reveals that this novel core–shell composite contains only Fe, C and O elements. An EA of α-Fe_2O_3@C shows that it contains C (12.34 wt%) and H (1.08 wt%), indicating that this core–shell material probably contains some organic functional groups, which is further confirmed by FT-IR (Fig. S3, *Supplementary data*). According to the spectrum, we find that C=O and C=C groups exist in α-Fe_2O_3@C core–shell composites, which supports the concept of aromatization of glucose during the hydrothermal reaction [19]. The peak at 3360 cm^{-1} implies the existence of residual hydroxyl groups and the peaks located at 3000–2850 cm^{-1} is the characteristic C–H stretches. The results reveal that there are lots of active function groups such as C=O, C=C and –OH groups in this core–shell composites, which will facilitate the linkage of catalytic species or biomolecules to the surface in the potential application [8,19,20].

The pod-like α-Fe_2O_3, sphere-like α-Fe_2O_3 and α-Fe_2O_3@C were explored as an additive to the thermal decomposition of ammonium perchlorate (AP), the key component of composite solid propellants. The TG and DTA curves of pure AP and AP in the presence of pod-like

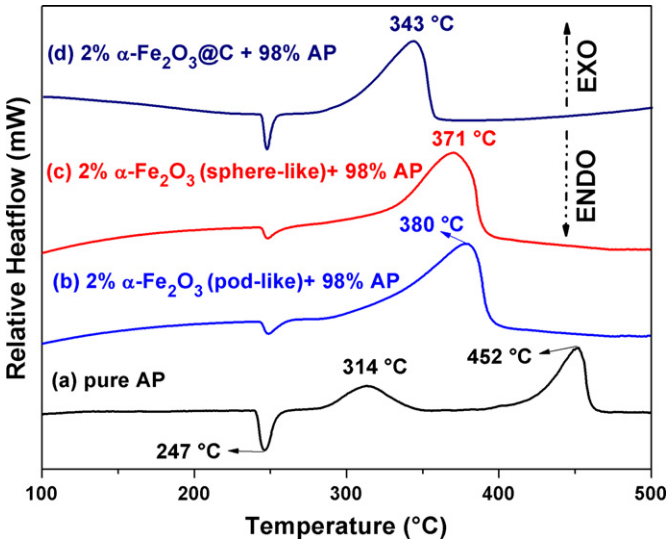

Fig. 3. DTA curves for: (a) pure AP; (b) pod-like α-Fe_2O_3 and AP; (c) sphere-like α-Fe_2O_3 and AP; and (d) α-Fe_2O_3@C and AP.

α-Fe_2O_3, sphere-like α-Fe_2O_3 and α-Fe_2O_3@C core–shell structure materials were, represented in Fig. S4 (*Supplementary data*) and Fig. 3. It can be observed from Fig. S4 that the addition of the as-obtained products in AP led to a significant reduction of the ending decomposition temperature of AP. Only two thermal signals can be observed for the mixture of AP and products, which compares to the three obvious peaks for pure AP. The first endothermic peak at 247 °C is

due to the crystal transformation of AP from an orthorhombic to cubic phase [21] and the additives have little effect on this crystallographic transition temperature. It is seen that there are two obvious exothermic peaks centered at about 314 and 452 °C on the DTA curve of pure AP (Fig. 3a), which are attributed to the low-temperature decomposition and high-temperature decomposition, respectively [21]. As seen in Fig. 3b–d, the low-temperature exothermic peak of AP decomposition has nearly disappeared. However, the high-temperature exothermic peak of AP shifts to a lower temperature at 380, 371 and 343 °C. From above analyses, it can be concluded that α-Fe_2O_3@C has higher catalytic activity towards the thermal decomposition of AP than that of α-Fe_2O_3, which is corresponding with the suggested result of FT-IR.

According to the previous reports [14,15,22], the decomposition of AP consists essentially of three steps:

(1) 240–250 °C: the crystal transformation from orthorhombic to cubic phase;
(2) 300–330 °C: the first decomposition step—a solid-gas multiphase reaction, including decomposition and sublimation shown as follows: $NH_4ClO_4 \rightarrow NH_4^+ + ClO_4^- \rightarrow NH_3(g) + HClO_4(g)$;
(3) 450–480 °C: the second decomposition step—NH_3 and $HClO_4$ react after entering the gas phase, and the products are N_2O, O_2, Cl_2, H_2O and few NO.

From our experimental results, we can deduce that the additives can catalytically decompose AP via the third step, because the temperature of the high-temperature exothermic decomposition process was reduced during the process, indicating that the catalytic mechanism is probably changed. According to the traditional electron-transfer theory [13,23], for one thing, the presence of partially filled 3*d* orbit in Fe^{3+} provides help in an electro-transfer process. Positive hole in an Fe_2O_3 can accept electrons from AP ion and its intermediate products enhancing the thermal decomposition of AP. So, the better catalytic activity of sphere-like α-Fe_2O_3 is attributed to its smaller particle sizes and more active sites, which are consistent with the previous Ref. [24]. For another thing, the amorphous carbon with aromatic structure containing lots of active function groups, such as C=C and C=O, is coated on the surface of α-Fe_2O_3, which might be helpful to electron transfer and heat conduction [10,25] and also can accelerate the thermal decomposition of AP. Thus, the α-Fe_2O_3@C core–shell composites have much higher catalytic activity towards the thermal decomposition of AP than that of α-Fe_2O_3.

4. Conclusion

In conclusion, sphere-like α-Fe_2O_3 with diameter about 25 nm and pod-like α-Fe_2O_3 with the major axis of about 314 nm and minor axis of about 137 nm have been selectively synthesized using $NH_3 \cdot H_2O$ and NaOH solution to adjust the pH value, respectively. The α-Fe_2O_3@C core–shell composites were fabricated by the coating experiments. The carbon shell is amorphous carbon with lots of active function groups, which promotes the catalytic performance of α-Fe_2O_3. The results of DTA illustrate that the decomposition temperatures of AP in the presence of pod-like α-Fe_2O_3, sphere-like α-Fe_2O_3 and α-Fe_2O_3@C are reduced to 72, 81 and 109 °C, respectively. Thus, the α-Fe_2O_3@C core–shell composites have much higher catalytic activity on the thermal decomposition of AP than that of α-Fe_2O_3, indicating the core–shell composites have better potential applications.

Acknowledgments

This work was partially supported by the National Science Fund for Fostering Talents in Basic Science (J0730426), Natural Science Foundation of Hubei Province (2005ABA034), Students' Scientific Research Program of Wuhan University (2007138), The Fourth Installment of Science and Technology Development 2010 Program of Suzhou (SYG201001) and Key Laboratory of Catalysis and Materials Science of Hubei Province (CHCL06003). We thank Mr. Shaobo Mo and Mrs. Ling Hu concerning the help of TEM and XRD.

Appendix A. Supplementary material

Supplementary data associated with this article can be found in the online version at doi:10.1016/j.jssc.2010.12.004.

References

[1] F. Caruso, Adv. Mater. 13 (2001) 11–22.
[2] Y. Wang, X.W. Teng, J.S. Wang, H. Yang, Nano Lett. 3 (2003) 789–793.
[3] X.M. Sun, J.F. Liu, Y.D. Li, Chem. Mater. 18 (2006) 3486–3494.
[4] S. Peng, J. Xie, S.H. Sun, J. Solid State Chem. 181 (2008) 1560–1564.
[5] L.-B. Luo, S.-H. Yu, H.-S. Qian, T. Zhou, J. Am. Chem. Soc. 127 (2005) 2822–2823.
[6] A. Odani, V.G. Pol, S.V. Pol, M. Koltypin, A. Gedanken, D. Aurbach, Adv. Mater. 18 (2006) 1431–1436.
[7] S.H. Xuan, L.Y. Hao, W.Q. Jiang, X.L. Gong, Y. Hu, Z.Y. Chen, Nanotechnology 18 (2007) 1–6.
[8] S.Y. Wu, Y.S. Ding, X.M. Zhang, H.O. Tang, L. Chen, B.X. Li, J. Solid State Chem. 181 (2008) 2171–2177.
[9] V.G. Pol, S.V. Pol, J.M. Calderon-Moreno, A. Gedanken, J. Phys. Chem. C 113 (2009) 10500–10504.
[10] X.J. Zhang, W. Jiang, D. Song, J.X. Liu, F.S. Li, Mater. Lett. 62 (2008) 2343–2346.
[11] L.P. Li, X.F. Sun, X.Q. Qiu, J.X. Xu, G.S. Li, Inorg. Chem. 47 (2008) 8839–8846.
[12] Y.P. Wang, J.W. Zhu, X.J. Yang, L.D. Lu, X. Wang, Thermochim. Acta 437 (2005) 106–109.
[13] Y.P. Wang, X.J. Yang, L.D. Lu, X. Wang, Thermochim. Acta 443 (2006) 225–230.
[14] L.M. Song, S.J. Zhang, B. Chen, J.J. Ge, X.C. Jia, Colloids Surf. A 360 (2010) 1–5.
[15] H. Xu, X.B. Wang, L.Z. Zhang, Powder Technol. 185 (2008) 176–180.
[16] S. Zhao, D. Ma, Preparation of $CoFe_2O_4$ nanocrystallites by solvothermal process and its catalytic activity on the thermal decomposition of ammonium perchlorate, J. Nanomater. Article ID 842816, (2010) (2010) 5 pages. doi:10.1155/2010/842816.
[17] V.A. Sadykov, L.A. Isupova, S.V. Tsybulya, S.V. Cherepanova, G.S. Litvak, E.B. Burgina, G.N. Kustova, V.N. Kolomiichuk, V.P. Ivanov, E.A. Paukshtis, A.V. Golovin, E.G. Avvakumov, J. Solid State Chem. 123 (1996) 191–202.
[18] R.B. Zheng, X.W. Meng, F.Q. Tang, J. Solid State Chem. 182 (2009) 1235–1240.
[19] X. Sun, Y. Li, Angew. Chem. Int. Ed. 43 (2004) 597–601.
[20] X.M. Sun, Y.D. Li, Adv. Mater. 17 (2005) 2626.
[21] V.V. Boldyrev, Thermochim. Acta 443 (2006) 1–36.
[22] L.J. Chen, L.P. Li, G.S. Li, J. Alloys Compd. 464 (2008) 532–536.
[23] A.A. Saida, R. Al-Qasmib, Thermochim. Acta 275 (1996) 83–91.
[24] L.L. Liu, F.S. Li, L.H. Tan, L. Ming, Y. Yi, Propell. Explos. Pyrot. 29 (2004) 34–38.
[25] L. Duclaux, Carbon 40 (2002) 1751–1764.